THE JOURNAL OF PHYSICAL CHEMISTRY A

Article

pubs.acs.org/JPCA

Multilayer Divide-Expand-Consolidate Coupled-Cluster Method: Demonstrative Calculations of the Adsorption Energy of Carbon Dioxide in the Mg-MOF-74 Metal−Organic Framework

Ashleigh L. Barnes,* Dmytro Bykov, Dmitry I. Lyakh, and Tjerk P. Straatsma

National Center for Computational Sciences, Oak Ridge National Laboratory, Oak Ridge, Tennessee 37831, United States

Supporting Information

ABSTRACT: The implementation and evaluation of a multilayer extension of the divide-expand-consolidate (DEC) scheme within the LSDalton program is presented. The DEC scheme is a linear-scaling, fragmentation-based local coupled-cluster (CC) method that provides a means of overcoming the scaling wall associated with canonical CC electronic structure calculations on large molecular systems. Taking advantage of the local nature of correlation effects, the correlation energy for the full molecule is calculated from a set of independent fragments using localized molecular orbitals. However, when only a small subsystem of a larger system is of interest, for example, adsorption sites or catalytically active sites, the majority of the computational time may be spent evaluating the correlation energy of fragments which have little effect on the properties in the area of interest (AOI). The multilayer DEC (ML-DEC) scheme addresses this by taking advantage of the independent nature of the fragments in order to evaluate the correlation energy of various regions of the system at different levels of theory. Regions far from the AOI are evaluated at lower (cheaper) levels of theory such as Hartree−Fock (HF) or Møller−Plesset second-order perturbation theory (MP2), while the area immediately surrounding the AOI is treated with a higher level CC model. Through the ML-DEC scheme, the computational cost of CC calculations on these types of systems can be significantly reduced while maintaining the accuracy of higher level calculations. Results from HF/RI-MP2 and RI-MP2/CCSD ML-DEC calculations of the binding energy of a fatty acid dimer are presented. We find that the ML-DEC scheme is capable of reproducing DEC energy differences at a target level of theory, provided that the region treated at the target level of theory is chosen to be sufficiently large. Time-to-solution is found to be significantly reduced, particularly in the RI-MP2/CCSD calculations. Finally, the ML-DEC scheme is applied to the calculation of CO_2 adsorption in a Mg-MOF-74 channel.

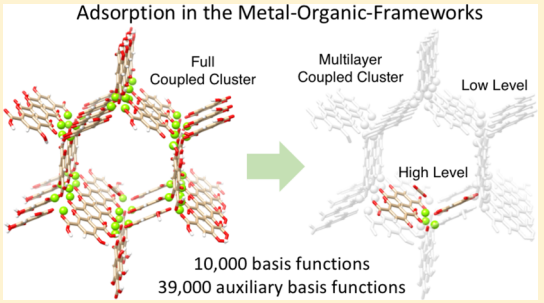

INTRODUCTION

In recent years, there has been a significant push to extend the applicability of high-accuracy coupled-cluster (CC) methods to larger systems, leading to the development of a number of local correlation schemes. Canonical CC methods treat correlation effects, which are mostly local by nature, within the delocalized Hartree−Fock (HF) basis resulting in $O(N^5)$ scaling with system size for the cheapest CC implementation, Møller−Plesset second-order perturbation theory (MP2), up to $O(N^7)$ for CC with singles, doubles, and perturbative triples excitations [CCSD(T)]. Local correlation schemes, however, utilize a localized basis for the calculation of correlation energies in order to overcome the scaling wall associated with canonical CC methods. These schemes are generally based on either the approximations of the wavefunction originating from the work of Pulay and Sæbø,[1−7] including the most efficient approximations based on pair natural orbital (PNO),[8−15] as well as other schemes based on local natural orbital (LNO)[16−18] or orbital-specific approximations,[19] or the approximations based on explicit fragmentation of the system. Fragmentation-based approaches, which include the fragment molecular orbital (FMO) method,[20,21] cluster-in-molecule (CIM) approach,[22−24] incremental method,[25−27] and divide-and-conquer scheme,[28,29] to name a few, are based on the work of Förner and co-workers[30,31] where the full-system CC correlation energy calculation is reduced into a set of smaller independent fragment CC calculations.

The divide-expand-consolidate (DEC) scheme[32−35] is one such fragmentation approach which relies on local occupied and virtual molecular orbitals (LMOs)[36] to calculate the correlation energy from a set of independent fragments. Unlike methods which rely on physical fragmentation of the system, such as FMO, the orbital space is only fragmented for the CC correlation calculation, while exchange interactions are still evaluated using canonical HF, therefore eliminating the need for many-body exchange calculations between fragments. Specifics of the DEC scheme will be discussed in the following section; however, the key feature that makes the DEC scheme unique among the fragmentation methods is that the fragments

Received: August 23, 2019
Revised: September 10, 2019
Published: September 12, 2019

DOI: 10.1021/acs.jpca.9b08077
J. Phys. Chem. A XXXX, XXX, XXX−XXX

are determined dynamically in an automated manner in order to ensure error control to a desired tolerance. The number of fragments increases linearly with the system size, making the DEC scheme linear-scaling overall. Fragment energies are evaluated independently, allowing for an embarrassingly parallel implementation with multiple levels of parallelism in order to improve load balancing. The end result is an algorithm poised to make efficient use of modern and upcoming supercomputing architectures.

In large systems, however, it is often the case that only a small region of the full system is of primary interest—for example, defects, adsorption sites, or catalytically active sites. In these cases, much of the computational effort in the DEC scheme is spent on evaluating the correlation energy of fragments which make a relatively small contribution to the property of interest. In these cases, the DEC scheme can be made more efficient by only applying high-level correlation methods, for example, CCSD or CCSD(T), to the regions of interest, while the remaining regions can be treated with lower level methods such as MP2 or HF.

Multilevel correlation approaches were first explored in the late 1990s. Perhaps the earliest example is the integrated molecular orbital + molecular orbital (IMOMO)[37] scheme introduced by Humbel, Sieber, and Morokuma, which allows for the combination of ab initio, density functional theory (DFT), or semiempirical MO methods for structure and energy prediction. This method was quickly followed by the ONIOM method,[38] which extended the two-layer IMOMO method to a three-layer approach combining CC, HF, or MP2 and force field methods.

Similarly, multilevel extensions to local correlation methods were pioneered in the local correlation schemes of Pulay and Sæbø and have since been implemented in a number of other local correlation schemes. For example, the local molecular orbital: molecular orbital method,[39] implemented by Mata, Werner, and Schütz, evaluates the correlation within regions of LMOs using different levels of Pulay's local correlation methods, for example, LCCSD(T) or LMP2. In this scheme, orbital pairs are assigned to the high or low level based on the atomic center to which they belong, and only strong pairs in which both orbitals fall within the high level region are evaluated at a high level. Another such multilevel scheme has been reported within the CIM approach[24] in which reactive sites within a system were treated using the completely renormalized CC method with singles, doubles, and non-iterative triples [CR-CC(2,3)][40,41] while remaining regions were treated with MP2. More recently, a multilevel approach was also implemented within the DLPNO-CCSD(T) method by imposing tighter accuracy thresholds for the local CCSD(T) calculations in regions of interest.[42] Also, a density-functional/wave-function embedding scheme based on LNOs was introduced by Kállay and co-workers.[43]

In this article, we report the implementation of a multilayer DEC (ML-DEC) scheme. The independent nature of the fragments within the DEC scheme allows for facile assignment of the fragments to different "layers" in which the correlation energy is evaluated at different levels of theory while maintaining the dynamic optimization of the fragments within user-controlled tolerances. To date, the ML-DEC scheme has been implemented and evaluated for any combination of HF, MP2, and CCSD (though it is recommended that the low level be only one step below the high level). In addition, the DEC scheme has recently been extended to include the resolution-of-the-identity MP2 (RI-MP2) model (DEC-RI-MP2)[44] as well as Laplace transformed RI-MP2 (DEC-LT-RIMP2).[45] These models significantly reduce the time-to-solution (TTS) of local MP2 calculations and are also available for use within the ML-DEC scheme.

As a proof of concept, we apply the ML-DEC scheme to the calculation of interaction energies in two different systems: (a) the palmitic acid ($C_{16}H_{32}O_2$) dimer and (b) CO_2 adsorbed on the open metal sites (OMS) of the metal−organic framework (MOF) Mg-MOF-74[46] (also known as CPO-27-Mg). The fatty acid dimer constitutes a simple test case to demonstrate the computational efficiency of the ML-DEC scheme as well as convergence of the ML-DEC correlation energy to the standard DEC energy as the high level layer expands. The interaction between the monomers is localized to the two carboxylic acid groups, making the initial assignment of the high-level layer straight forward, and expansion of the high level layer requires only progressing along the carbon chains.

The MOF system, on the other hand, provides a test of the ML-DEC scheme in a larger and more complex environment. The choice of this test system is motivated by recent investigations into the effects of acid gases on MOFs in the context of carbon sequestration from industrial flue gas. MOFs with OMSs such as Mg-MOF-74 have been studied for this purpose due to their high adsorption capacity for CO_2. However, acid gases such as SO_x and NO_x, along with H_2O, are found as impurities in flue gas, and these compete heavily for adsorption sites within the MOF, effectively poisoning the material. Understanding the effects of these acid gases requires the characterization of their interactions with MOFs through both experimental and computational means. Traditionally, these interactions have been studied computationally in periodic MOF systems using plane-wave DFT; however, the results of these calculations are highly dependent on the choice of pseudopotential and additional parameters such as Hubbard-*U* corrections and van der Waals dispersion corrections. In the absence of corresponding experimental data, it is impossible to know with certainty which parameterizations provide the most realistic description of the MOF-adsorbate interaction. It is therefore desirable to use methods within the hierarchy of CC theory which account for dispersion and can be systematically improved by increasing the level at which correlation is treated. However, because of the high computational cost of the CC methods, this typically limits the computational investigations to small clusters which suffer from errors due to finite size effects.

In order to capture the chemical environment within the MOF, larger clusters than those accessible to canonical CC methods must be used, and therefore, these systems stand to benefit greatly from the linear-scaling, embarrassingly parallel DEC scheme. In addition, it is well established from previous experimental and theoretical investigations that the strongest interactions between Mg-MOF-74 and the adsorbate gas molecules generally occur at the OMSs.[47−51] This suggests that we can efficiently evaluate the adsorption energies of these small gas molecules within the MOF using the ML-DEC scheme by treating only the fragments centered on the adsorbate, OMSs, and the immediate neighbors at the high level of theory while all other fragments are evaluated at the low level. However, we wish to emphasize that the calculations presented here are intended to demonstrate the capability of the ML-DEC scheme to efficiently treat large systems with the accuracy of standard DEC calculations rather than to obtain

DOI: 10.1021/acs.jpca.9b08077
J. Phys. Chem. A XXXX, XXX, XXX−XXX

adsorption energies with experimental accuracy. We have therefore used a relatively simple method to optimize the placement of the CO_2 molecule within the MOF channel rather than performing extensive optimizations on the periodic system. For the same reason, basis set superposition error (BSSE) corrections have also not been included.

This manuscript is organized as follows: we first briefly review the DEC scheme and describe the implementation of the ML-DEC scheme. Next, results of HF/RI-MP2 and RI-MP2/CCSD ML-DEC test calculations on the palmitic acid dimer are reported, which are compared to standard DEC calculations. We then discuss the application of the ML-DEC scheme to the calculation of the CO_2 adsorption energy in a 793-atom Mg-MOF-74 channel. Finally, conclusions regarding the efficiency and accuracy of the ML-DEC scheme are provided.

THEORY

Review of the DEC Scheme. Here, we present a brief review of the DEC scheme as implemented in the LSDalton program[52] within the Dalton suite.[53] For a more detailed description of the DEC scheme, the reader is referred to refs.[32,34]

As mentioned above, the DEC scheme and other local correlation methods rely on LMOs in order to overcome the steep scaling of canonical CC methods. In the DEC scheme, canonical occupied and virtual MOs (CMOs) are first obtained from a canonical HF calculation on the full system. Fragmentation of the orbital space is only introduced in the correlation calculation. The CMOs are then localized to obtain the set of LMOs which are assigned to the nearest atom relative to the center of charge of each LMO. By default, orbitals centered on light atoms (i.e., hydrogen) are assigned to the nearest heavy atom. A number of localization schemes have been implemented in LSDalton, including Pipek−Mezey,[54] Boys,[55] and powers of the second[56] and fourth[57] central moments (PSM and PFM, respectively). The calculations presented here utilized the PSM method with powers of 2 for both occupied and virtual orbital localization. A review of these localization schemes can be found in ref 36.

The DEC scheme is based on the decomposition of the correlation energy of a molecular system into the sum of atomic and pair correlation energies within the system

$$E_{\mathrm{corr}} = \sum_{P}^{N_{\mathrm{frag}}} \left[E_P + \frac{1}{2} \sum_{Q \neq P}^{N_{\mathrm{frag}}} \Delta E_{PQ} \right] \tag{1}$$

Letting i,j represent occupied orbitals and a,b represent virtual orbitals, E_P and ΔE_{PQ} in the above equation can be written in terms of electron repulsion integrals (g) and CC amplitudes (t) according to eqs 2 and 3 below.

$$E_P = \sum_{ij \in P} \sum_{ab} (t_{ij}^{ab} + t_i^a t_j^b)(2g_{iajb} - g_{ibja}) \tag{2}$$

$$\Delta E_{PQ} = \sum_{i \in P, j \in Q} \sum_{ab} (t_{ij}^{ab} + t_i^a t_j^b)(2g_{iajb} - g_{ibja}) + \sum_{i \in Q, j \in P} \sum_{ab} (t_{ij}^{ab} + t_i^a t_j^b)(2g_{iajb} - g_{ibja}) \tag{3}$$

The above formulations of the correlation energy introduce no approximations. However, in order to achieve linear scaling, we truncate the virtual orbital space for each fragment and introduce a distance cutoff, R_{cut}, to eliminate pairs of fragments separated by large distances where correlation would be negligible. With these approximations, eqs 2 and 3 become

$$E_P = \sum_{ij \in P} \sum_{ab \in [\bar{P}]} (t_{ij}^{ab} + t_i^a t_j^b)(2g_{iajb} - g_{ibja}) \tag{4}$$

$$\Delta E_{PQ} = \sum_{\substack{i \in P, j \in Q \\ ab \in [\bar{P}] \cup [\bar{Q}] \\ R_{PQ} < R_{\mathrm{cut}}}} (t_{ij}^{ab} + t_i^a t_j^b)(2g_{iajb} - g_{ibja}) + \sum_{\substack{i \in Q, j \in P \\ ab \in [\bar{P}] \cup [\bar{Q}] \\ R_{PQ} < R_{\mathrm{cut}}}} (t_{ij}^{ab} + t_i^a t_j^b)(2g_{iajb} - g_{ibja}) \tag{5}$$

where $[\bar{P}]$ and $[\bar{Q}]$ represent the truncated virtual orbital spaces (in the LMO basis) of fragments P and Q, respectively, and R_{PQ} is the distance between the atomic centers of the two fragments. $[\bar{P}]$ and $[\bar{Q}]$ are optimized self-consistently in order to ensure error control to a user-defined tolerance, denoted the fragment optimization threshold or FOT (default value: 1×10^{-4} E_h).

Reference 58 provides a detailed description of the stages of fragment optimization which we briefly discuss here. The optimization of an atomic fragment's virtual orbital space $[\bar{P}]$ is accomplished in two steps: fragment expansion and fragment reduction. During fragment expansion, sets of virtual orbitals localized to neighboring atomic sites are sequentially added to $[\bar{P}]$ according to a priority list based on the distance between the atomic center of fragment P and the center of charge of a given orbital. As groups of orbitals are added, the atomic fragment energy is evaluated and expansion continues until the change in energy from the previous expansion step is less than the FOT. Fragment reduction is then performed to determine if any orbitals can be removed from $[\bar{P}]$ without introducing errors larger than the FOT. This step is necessary in order to improve the computational efficiency of the pair fragment calculations, which will be discussed next. Both fragment expansion and reduction are iterative processes that require the evaluation of the atomic fragment correlation energy after each iteration and therefore fragment optimization is typically performed using a less expensive method such as MP2 or RI-MP2. In the final step of fragment reduction, the MP2 or RI-MP2 optimized atomic fragment energies are obtained. If this corresponds to the DEC target level of theory, no further calculations of the atomic fragments are required. Otherwise, if a higher level of theory is requested, the atomic fragment correlation energies are reevaluated according to eq 2 using the optimized $[\bar{P}]$ at the target level of theory.

The truncated virtual orbital spaces for pair fragments are constructed from the union of the constituent optimized atomic fragments, $[\bar{P}] \cup [\bar{Q}]$. This highlights the need for the reduction step in the fragment optimization procedure as any reduction of $[\bar{P}]$ and $[\bar{Q}]$ similarly reduces the virtual orbital space for every pair involving those atoms. As there are many more pair fragment calculations than atomic fragment calculations to perform and pair fragments inherently involve much larger orbital spaces, reduction in the cost of evaluating

DOI: 10.1021/acs.jpca.9b08077
J. Phys. Chem. A XXXX, XXX, XXX−XXX

the pair correlation energies can provide significant improvements in the overall computational efficiency as well as memory requirements for individual fragments. The cost of the pair calculations is also reduced through a screening method in which pair energies are estimated using partially optimized atomic virtual orbital spaces. The lowest energy pairs whose total estimated energy does not exceed the FOT are omitted from the optimized pair fragment calculations. The pair energy estimations are typically performed at the same level of theory as fragment expansion and reduction.

Following the optimization steps and pair energy estimation, atomic and pair fragment energies are evaluated for the optimized fragments at the target level of theory as necessary. These individual fragment energies are added according to eq 1 to provide the total correlation energy correction to the canonical HF energy. Errors bound by the FOT per atomic fragment are introduced in both the fragment optimization step and pair energy estimate calculations, and therefore, the overall error in the DEC scheme is approximated by

$$\delta E_{\mathrm{DEC}} = 2 \times \mathrm{FOT} \times N_{\mathrm{frag}} \tag{6}$$

Coarse, medium, and fine-grained parallelism is utilized in order to achieve computational efficiency in the DEC scheme. Fragments are evaluated independently by groups of processors which distribute the calculation over multiple nodes using MPI. Within the nodes, work is further divided using OpenMP or OpenACC.

ML-DEC Scheme. In this section, we discuss the implementation of the ML-DEC scheme, which is included in the LSDalton2018.0 release. The ML-DEC scheme takes advantage of the independent nature of the fragment calculations which allows for the evaluation of fragment correlation energies at different levels of theory. The layers are defined by the user by assigning atoms in the MOLECULE.INP file to level = high or level = low. This is visualized in Figure 1, in which a large molecular system has been subdivided into two layers: a high level layer (yellow) and a low level layer (blue). Correlation energies of the atomic fragments are evaluated based on the level into which their atomic center has been assigned. It is important to note that the user-defined layers are not required to be contiguous as shown in Figure 1, making the ML-DEC scheme suited to treat more complex problems such as multisite catalysis. Although chemical intuition on the part of the user is required to assign atoms to the high- and low-level layers, this method maintains the user-friendly, automatic fragment optimization governed by the FOT as in the standard DEC scheme.

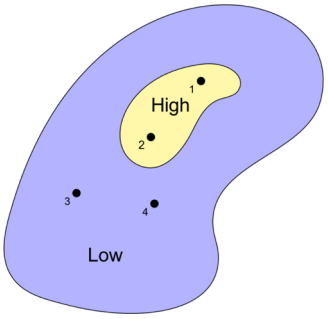

Figure 1. Visualization of high (yellow) and low (blue) level layers in the ML-DEC scheme. Black dots labeled 1−4 denote centers of representative atomic fragments.

The ML-DEC scheme begins with the same atomic fragment optimization and pair energy estimation steps as in the standard DEC scheme, described above. All atomic fragments are optimized at the same level of theory, regardless of their assignment to the high or low level layers. After fragment optimization, target CC models are assigned to each atomic fragment according to the user specifications. Pair fragments are evaluated at the higher of the levels of theory requested for the two constituent atomic fragments. For example, in Figure 1 above, the pair between atoms 1 and 2 would be evaluated at the high level of theory, pair between atoms 2 and 3 would be evaluated at the high level of theory, and pair between atoms 3 and 4 would be evaluated at the low level of theory. As in the standard DEC scheme, computational efficiency is improved by omitting pair fragment calculations whose correlation energies do not contribute significantly to the total correlation energy based on the pair energy estimates. However, pair fragments from the high level layer which should be skipped based on their energy estimates are instead reduced to the low level layer. Finally, all atomic and pair fragments whose energies have not been evaluated at their target levels of theory during the optimization process are evaluated, and the total correlation energy is obtained according to eq 1 as before.

Example LSDALTON.INP and MOLECULE.INP input files for a number of ML-DEC calculations are provided in the Supporting Information along with descriptions of parameters which users may adjust in order to improve computational efficiency of the ML-DEC calculations. Current CC models integrated within the ML-DEC scheme are MP2, RI-MP2 [with and without the use of Laplace transformations (LT)], CCSD, and CCSD(T), though ML-DEC calculations utilizing CCSD(T) have not yet been evaluated for efficiency and accuracy against standard DEC-CCSD(T) calculations. In addition, the low-level layer may be treated at the HF level of theory, ignoring correlation effects. It is recommended that only one level of theory separate the high and low levels.

Simulations treating the low-level layer with HF require a few special considerations in order to improve computational efficiency. Although correlation contributions from atoms in the low level should not be calculated, the atoms may still contribute to pairs with high-level atoms, requiring optimization of these atomic fragments. In order to reduce the number of fragment optimizations that must be performed, we utilize the existing pair threshold cutoff R_{cut} to determine which atomic fragments can be safely omitted from the optimization steps. All low-level atoms within R_{cut} of any high level atom will be optimized while the remaining low-level atomic fragments are skipped. For most applications, R_{cut}, corresponding to the input keyword .PAIRTHR or .PAIRTHRANGSTROM, of about 10.0 Å is sufficient as correlation effects fall off significantly beyond this distance. Because the atomic fragment correlation energies at the level of theory used for fragment reduction are obtained automatically from the optimization procedure, contributions from optimized low-level atomic fragments in HF/RI-MP2 ML-DEC calculations are accounted for at no additional computational cost.

The ML-DEC scheme is expected to be particularly beneficial in the calculation of interactions localized to small, isolated areas within the system, as errors from correlation effects in the low-level layers far from regions of interest are

DOI: 10.1021/acs.jpca.9b08077
J. Phys. Chem. A XXXX, XXX, XXX−XXX

expected to cancel out when monomer energies are subtracted from the interacting system. Accurate results do of course depend on effective partitioning of the system into high- and low-level layers. In the following section, we will discuss convergence of calculated interaction energies with the size of the high level layer in the palmitic acid dimer test system, as well as resulting effects on the computational efficiency.

RESULTS AND DISCUSSION

Test Case 1: Palmitic Acid Dimer. As a first test of the ML-DEC scheme we consider the palmitic acid dimer. The interaction between the two monomers in this system is localized to the carboxylic acid groups through the formation of hydrogen bonds. It is therefore a reasonable approach to assign the −COOH group of each monomer to the high level layer, and this was taken as the initial configuration in both HF/RI-MP2 and RI-MP2/CCSD ML-DEC calculations as shown in Figure 2. This will be referred to as the minimal high-level layer. In order to demonstrate convergence to the standard DEC scheme reference energy, we also consider two extended high level layers which include one or two additional carbon atoms per monomer (shown in blue in Figure 2). Both the monomer and dimer systems used for these calculations were optimized at the DFT level of theory using the BP86 functional[59,60] and the cc-pVTZ basis set as implemented in NWChem.[61]

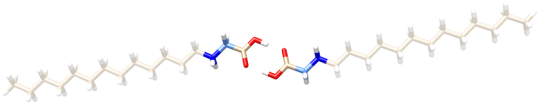

Figure 2. Palmitic acid dimer optimized using DFT with the BP86 functional and the cc-pVTZ basis set. Opaque atoms are those included in the high-level layer: red = oxygen, white = hydrogen, tan = carbon included in minimal high level layer, light blue = carbon included in first extension of the high level layer (ext_1), dark blue = carbon included in second extension of the high level layer (ext_2).

HF/RI-MP2 Calculations. DEC-RI-MP2 and HF/RI-MP2 ML-DEC calculations on the palmitic acid dimer utilize the cc-pVTZ basis set for all atoms and FOT = 1×10^{-4} E_h. The binding energy, ΔE is calculated from independent energy calculations of the optimized monomer and the optimized dimer system according to eq 7

$$\Delta E = E_D^D(D) - 2 \times E_M^M(M) \quad (7)$$

where D and M denote the dimer and monomer systems, respectively, and $E_X^Y(Z)$ is the energy of system Z in the optimized geometry of system X in the basis of system Y. A consistent assignment of high level atoms is maintained in the monomer and dimer calculations, and a cutoff of R_{cut} = 10.0 Å is used to reduce the number of fragment optimization calculations. The number of RI-MP2 fragment optimization calculations as well as final pair energy calculations are summarized in Table 1 for the minimal high level layer (−COOH on each monomer) and each extended high level layer. We note that BSSE corrections have not been applied to the interaction energies. However, their calculation via the counterpoise correction (CPC) is straightforward and does not differ from corrections calculated using the standard DEC scheme. The CPC requires an additional HF/localization calculation of each monomer in the presence of the ghost atoms of the other monomer and, for the ML-DEC scheme, consistent assignment of atoms to high- and low-level layers.

Table 1. Fragment Optimization and Pair Energy Calculations Performed during Palmitic Acid Monomer and Dimer DEC-RI-MP2 and HF/RI-MP2 ML-DEC Calculations[a]

model	fragment optimizations	pair energy calculations
Monomer, 988 Basis Functions		
ML-DEC	9	6
ML-DEC (ext_1)	10	9
ML-DEC (ext_2)	11	12
DEC-RI-MP2	17	51
Dimer, 1976 Basis Functions		
ML-DEC	20	32
ML-DEC (ext_1)	22	42
ML-DEC (ext_2)	24	50
DEC-RI-MP2	36	130

[a]ML-DEC (ext_1) refers to ML-DEC calculation utilizing a high level layer including one additional carbon atom per monomer (i.e., $-CH_2COOH$), and ML-DEC (ext_2) refers to a high level layer with two additional carbon atoms per monomer (i.e., $-CH_2CH_2COOH$).

Performance of these simulations is evaluated based on TTS of the monomer and dimer calculations (TTS_m and TTS_d, respectively) for the ML-DEC scheme compared to the standard DEC scheme at the RI-MP2 level of theory. The same number of processors were used in the DEC and ML-DEC calculations, and care was taken to ensure that the number of MPI groups (an MPI group is a set of MPI processes assigned to one DEC fragment) did not exceed the number of fragment calculations in either the optimization or final energy calculation stages of the simulation so that processors were not sitting idle. Table 2 reports the energies and TTS obtained for both monomer and dimer DEC and ML-DEC calculations.

Table 2. Palmitic Acid Dimer Binding Energies from HF/RI-MP2 ML-DEC and DEC-RI-MP2 Simulations[a]

model	TTS_m (min)	TTS_d (min)	ΔE (kJ/mol)
ML-DEC	6.71	5.51	−87.7
ML-DEC (ext_1)	7.98	6.21	−69.6
ML-DEC (ext_2)	9.27	6.84	−70.6
DEC-RI-MP2	17.51	10.19	−70.4

[a]TTS is reported for both the monomer (TTS_m) and dimer (TTS_d). DEC and ML-DEC monomer calculations were run on 7 processors, while dimer calculations used 33. Energies are reported in kJ/mol.

From the results in Table 2, we can conclude that the ML-DEC scheme results in a significant decrease in TTS_m and TTS_d, reducing the full TTS by about half for the minimal high level layer. It is important to note that for RI-MP2 calculations, the majority of the simulation time is typically spent in fragment optimization, which requires multiple RI-MP2 level calculations on each atomic fragment through the expansion and reduction procedures. Therefore, reduction in the number of fragment optimizations (Table 1) has a more significant impact on the computational time than reductions in the number of pair fragments. For this reason, the ratio between TTS_m for the DEC and ML-DEC calculations lies closer to the ratio between their respective number of fragment optimizations rather than pair energy calculations.

DOI: 10.1021/acs.jpca.9b08077
J. Phys. Chem. A XXXX, XXX, XXX−XXX

In addition to this substantial reduction in computational time, we find that after the first extension of the high level layer [ML-DEC (ext_1)], HF/RI-MP2 ML-DEC calculations are able to reproduce the reference DEC-RI-MP2 interaction energies within 2%. Further extending the high level layer [ML-DEC (ext_2)] increases the TTS slightly while bringing the binding energy into nearly exact agreement with the DEC-RI-MP2 reference (within 0.3%). This rapid convergence to the DEC-RI-MP2 reference value demonstrates that as we move away from the center of these local interactions, correlation effects from more remote fragments make a negligible contribution to the interaction.

RI-MP2/CCSD Calculations. It is expected that more rapid convergence to the reference DEC binding energy can be obtained when a low-level model which includes correlation effects is utilized. In order to verify this, the binding energy of the palmitic acid dimer has been evaluated using both RI-MP2/CCSD ML-DEC and standard DEC-CCSD calculations with the cc-pVDZ basis set and FOT = 1×10^{-4} E_h. For these simulations, the RI-MP2 level fragment optimizations no longer dominate the computational time and therefore reduction in the TTS can be better predicted by the reduction in CCSD-level pair energy calculations as shown in Table 3. Only the minimal high-level layer investigated above is used for the RI-MP2/CCSD ML-DEC calculations.

Table 3. Simulation Size and Performance Data for RI-MP2/CCSD ML-DEC and DEC-CCSD Calculations on the Palmitic Acid Dimer[a]

	CCSD pair fragment calculations		TTS		
model	monomer	dimer	monomer (h)	dimer (h)	ΔE (kJ/mol)
ML-DEC	14	38	0.24	1.85	−70.2
DEC-CCSD	76	164	3.21	8.40	−69.4

[a]All simulations were run on 129 processors with 8 threads per process.

From the TTS data provided in Table 3, it is apparent that the computational savings are much more significant for RI-MP2/CCSD than HF/RI-MP2 because the bottleneck is no longer fragment optimization. In addition, even the smallest high level layer results in agreement within 2% of the reference DEC-CCSD energy. This is to be expected because the correlation energy of low level fragments is still being accounted for, though at the RI-MP2 level rather than CCSD, and the energy difference between CCSD and RI-MP2 is less than that between RI-MP2 and HF. Comparing to the DEC-RI-MP2 binding energy calculated with the cc-pVDZ basis set, −74.8 kJ/mol, we see that the RI-MP2/CCSD ML-DEC energy captures approximately 85% of the energy difference between the DEC-CCSD and DEC-RI-MP2 binding energies while reducing the TTS for the monomer and dimer calculations by 92.5 and 78.0%, respectively, compared to the full DEC-CCSD calculations.

Test Case 2: CO_2 Adsorption in Mg-MOF-74. The results discussed in the previous section demonstrate the computational efficiency of the ML-DEC scheme and its accuracy with respect to the standard DEC scheme, given a sufficiently large high level layer. We now apply the ML-DEC scheme to a more industrially relevant real-world problem, CO_2 adsorption in Mg-MOF-74.

The MOF-74 isostructural family is made up of M^{2+} metal ions (M = Mg, Co, Ni, Zn) coordinated by dobdc = 2,5-dioxido-1,4-benzene-dicarboxylate ligands with an overall formula of M_2 (dobdc). Each metal center is coordinated by five dobdc oxygen atoms in an approximately square pyramidal configuration. The resulting open metal site has been shown to play a crucial role in strong binding affinities for a number of small gas molecules. In particular, Mg-MOF-74 has been shown experimentally to adsorb CO_2 with an uptake at 1.02 bar of 6.18 mmol/g.[62] Adsorption energies have previously been calculated in periodic models of Mg-MOF-74 via plane-wave DFT[63] as well as in small cluster models via molecular DFT and MP2;[64] however, the calculated adsorption energies vary by over 10 kJ/mol depending on the method and system size. DFT results are particularly susceptible to influence from the choice of functionals, dispersion corrections, and plane-wave cutoff energies, among other adjustable parameters, while cluster models inevitably suffer from edge effects. By applying the ML-DEC scheme to the calculation of the CO_2 adsorption energy in a large, finite Mg-MOF-74 cluster, we can explicitly treat correlation near the adsorption site and minimize edge effects, thereby addressing many of the sources of variability listed above.

For these calculations, we use a 793-atom Mg-MOF-74 channel with a single adsorbed CO_2 molecule as shown in Figure 3. Details of the geometry optimization are provided in the Supporting Information. A minimal high level layer is first considered which contains only the Mg onto which the CO_2 is adsorbed, five coordinating oxygen atoms, and CO_2 molecule (Figure 4a). The high-level layer is expanded until the calculated interaction energy converges to the standard DEC-RI-MP2 energy. However, for this system, expansion of the high-level layer is not as straightforward as in the palmitic acid dimer test case as there are a number of different ways in which the high level layer can be expanded. As a first approach, we select all MOF atoms within 5 Å of the adsorbed CO_2 molecule to include in the expanded high level layer. Care is taken not to divide resonant structures across layers, and therefore, if any part of an aromatic ring falls within the 5 Å region, the full aromatic ring is included in the high-level layer. For the second expansion, terminal phenyl and carboxyl groups

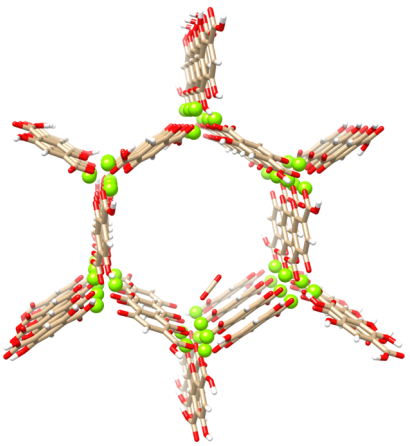

Figure 3. Mg-MOF-74 channel with a single adsorbed CO_2 molecule. Green = Mg, red = O, tan = C, white = H.

DOI: 10.1021/acs.jpca.9b08077
J. Phys. Chem. A XXXX, XXX, XXX−XXX

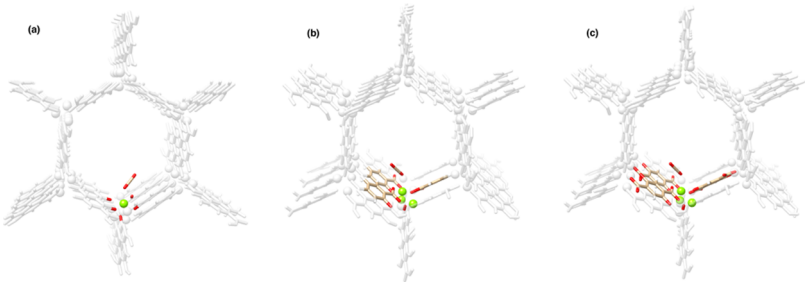

Figure 4. Mg-MOF-74 + CO_2 minimal high level layer (a), along with the first (b) and second (c) extensions to the high level layer for ML-DEC calculations. High-level atoms are shown in color (green = Mg, red = O, tan = C) and all low-level atoms are shown in white.

on the aromatic rings included in the first expansion are added to the high-level layer. The two expanded high-level layers are shown in Figure 4b,c.

Calculations on the MOF channel and its adsorbate utilize the cc-pVDZ basis set on all atoms, a pair threshold cutoff of 10.0 Å and FOT = 1×10^{-5} E_h. The same localized HF MOs are used in both the standard DEC and ML-DEC calculations. As a comparison of the efficiency of these calculations, the number of fragment optimization and pair energy calculations required for the various HF/RI-MP2 ML-DEC models as well as the DEC-RI-MP2 model are summarized in Table 4. From

Table 4. Atomic Fragment Optimizations and Optimized Pair Energy Calculations Performed during HF/RI-MP2 ML-DEC and Standard DEC-RI-MP2 Calculations on the Mg-MOF-74 + CO_2 System[a]

model	fragment optimizations	pair energy calculations
ML-DEC	202	566
ML-DEC (ext_1)	282	2005
ML-DEC (ext_2)	323	2728
DEC-RI-MP2	568	14 720

[a]The model ML-DEC refers to the ML-DEC calculations using the minimal high level layer as shown in Figure 4a while ML-DEC (ext_1) and ML-DEC (ext_2) refer to the first and second extensions of the high level layer as shown in Figure 4b,c, respectively.

this information, we see that even for the largest high level layer, ML-DEC (ext_2), the number of atomic fragment optimization steps is reduced by more than 40% while the pair energy calculations are reduced by over 80%. This indicates the potential for even greater computational savings in RI-MP2/CCSD and CCSD/CCSD(T) ML-DEC calculations on these systems.

The interaction energies (ΔE) obtained from each of the models in Table 4 are calculated according to eq 8

$$\Delta E = E^{\mathrm{MOF+CO_2}}_{\mathrm{MOF+CO_2}}(\mathrm{MOF} + \mathrm{CO_2}) - E^{\mathrm{MOF}}_{\mathrm{MOF+CO_2}}(\mathrm{MOF}) - E^{\mathrm{CO_2}}_{\mathrm{MOF+CO_2}}(\mathrm{CO_2}) \quad (8)$$

where as before $E^{Y}_{X}(Z)$ is the energy of system Z in the optimized geometry of system X on the basis of system Y. We note that this equation differs from eq 7 in that the energies of the monomers are evaluated in the geometry of the complex, thus providing the interaction energy rather than the binding energy. For this study, no correction for BSSE was made. The resulting interaction energies are reported in Table 5. It should be noted that the results presented here are primarily intended to demonstrate that ML-DEC interaction energies rapidly converge to standard DEC values. Reproducing experimental

Table 5. Interaction Energies (ΔE) from DEC-RI-MP2 and HF/RI-MP2 ML-DEC Calculations on the Mg-MOF-74 + CO_2 System[a]

model	ΔE (kJ/mol)	|error| (kJ/mol)
DEC-RI-MP2	−68.5	
ML-DEC	−4147.0	4078.5
ML-DEC (ext_1)	−647.7	579.2
ML-DEC (ext_2)	−72.4	3.9

[a]Errors in the ML-DEC values with respect to the standard DEC-RI-MP2 value are reported as well.

adsorption data would require either a larger basis set or BSSE corrections, along with a more rigorous initial geometry optimization of the system. Nevertheless, our results are in qualitative agreement with previous theoretical studies at DFT[63,64] and MP2[64] levels of theory, which range from −45 to −54 kJ/mol.

The results presented in Table 5 demonstrate that the minimal high level layer consisting of the central Mg atom, its five coordinating oxygen atoms, and the CO_2 molecule does not sufficiently capture the important correlation effects in the CO_2−MOF interaction. However, as the high level layer expands, the ML-DEC interaction energy converges rapidly to the DEC-RI-MP2 energy. Agreement within 6% between the HF/RI-MP2 ML-DEC and DEC-RI-MP2 interaction energies is obtained when the terminal carboxyl and phenyl functional groups on these ligands are also included in the high level layer. This model, ML-DEC (ext_2), is therefore considered to be the optimal multilayer configuration for the MOF + CO_2 system. Using this multilayer configuration, we are able to calculate the RI-MP2 interaction energy of this approximately 10 000 basis function system with significantly less computational effort than required for a standard DEC-RI-MP2 calculation without loss of accuracy. The ML-DEC runs were performed using smaller node count and thus direct comparison of TTS is not possible. Nevertheless, based on the number of fragment evaluations presented in Table 4, we expect a factor of 3 performance gain from using the ML-DEC approach.

CONCLUSIONS

Through the test cases presented above, we have demonstrated that interaction energies calculated using the ML-DEC scheme agree with the results obtained from standard DEC calculations at the higher level of theory while reducing the overall TTS. By exploiting the rapid drop-off of correlation energy with distance, important contributions to a local interaction can be captured at a high level of theory while significantly decreasing the number of atomic and pair

DOI: 10.1021/acs.jpca.9b08077
J. Phys. Chem. A XXXX, XXX, XXX−XXX

fragment energies that must be evaluated at that level. The improved computational efficiency of the ML-DEC scheme allows for the treatment of much larger systems than those reasonably accessible with the standard DEC scheme, which has important implications for large systems in which the process or interaction of interest can be localized to isolated regions within the overall system, for example, defect sites, adsorption sites, or catalytically active sites.

We have shown that the accuracy of the ML-DEC scheme relative to standard DEC calculations depends on proper assignment of atoms to the high level layer which requires some chemical intuition; however, a conservative high level layer may be obtained through optimization at the less expensive HF/RI-MP2 ML-DEC level for use in subsequent RI-MP2/CCSD or, potentially, CCSD/CCSD(T) calculations. In addition, these optimized high-level layers can provide qualitative information on the extent of important correlation effects in a given system.

Overall, the ML-DEC scheme provides a powerful tool for the evaluation of interactions within large systems, such as biologically or industrially relevant materials, at CC levels of theory.

■ ASSOCIATED CONTENT

Supporting Information

The Supporting Information is available free of charge on the ACS Publications website at DOI: 10.1021/acs.jpca.9b08077.

Example LSDALTON.INP and MOLECULE.INP files as well as details of the optimization of the Mg-MOF-74 channel (PDF)

■ AUTHOR INFORMATION

Corresponding Author

*E-mail: alocke5@vols.utk.edu.

ORCID

Ashleigh L. Barnes: 0000-0001-6793-7699

Notes

The authors declare no competing financial interest.

■ ACKNOWLEDGMENTS

This research used resources of the Oak Ridge Leadership Computing Facility (OLCF), which is a DOE Office of Science User Facility supported under Contract DE-AC05-00OR22725. The work was performed as part of an effort to ready scientific applications for effective use of OLCF's Summit supercomputer within the Center for Accelerated Application Readiness (CAAR), and the authors acknowledge Early Science Project access to Summit. This work was supported in part by UNCAGE-ME, an Energy Frontier Research Center funded by the U.S. Department of Energy, Office of Science, Basic Energy Sciences under award no. DE-SC0012577.

■ REFERENCES

(1) Pulay, P. Localizability of Dynamic Electron Correlation. *Chem. Phys. Lett.* **1983**, *100*, 151−154.

(2) Sæbø, S.; Pulay, P. Local Configuration Interaction: An Efficient Approach for Larger Molecules. *Chem. Phys. Lett.* **1985**, *113*, 13−18.

(3) Pulay, P.; Sæbø, S. Orbital-Invariant Formulation and Second-Order Gradient Evaluation in Møller-Plesset Perturbation Theory. *Theor. Chim. Acta* **1986**, *69*, 357−368.

(4) Saebø, S.; Pulay, P. Fourth-Order Møller-Plessett Perturbation Theory in the Local Correlation Treatment. I. Method. *J. Chem. Phys.* **1987**, *86*, 914−922.

(5) Saebo, S.; Pulay, P. The Local Correlation Treatment. II. Implementation and Tests. *J. Chem. Phys.* **1988**, *88*, 1884−1890.

(6) Saebo, S.; Tong, W.; Pulay, P. Efficient Elimination of Basis Set Superposition Errors by the Local Correlation Method: Accurate Ab Initio Studies of the Water Dimer. *J. Chem. Phys.* **1993**, *98*, 2170−2175.

(7) Saebo, S.; Pulay, P. Local Treatment of Electron Correlation. *Annu. Rev. Phys. Chem.* **1993**, *44*, 213−236.

(8) Riplinger, C.; Sandhoefer, B.; Hansen, A.; Neese, F. Natural Triple Excitations in Local Coupled Cluster Calculations with Pair Natural Orbitals. *J. Chem. Phys.* **2013**, *139*, 134101.

(9) Riplinger, C.; Neese, F. An Efficient and Near Linear Scaling Pair Natural Orbital Based Local Coupled Cluster Method. *J. Chem. Phys.* **2013**, *138*, 034106.

(10) Riplinger, C.; Pinski, P.; Becker, U.; Valeev, E. F.; Neese, F. Sparse maps-A systematic infrastructure for reduced-scaling electronic structure methods. II. Linear scaling domain based pair natural orbital coupled cluster theory. *J. Chem. Phys.* **2016**, *144*, 024109.

(11) Schwilk, M.; Ma, Q.; Köppl, C.; Werner, H.-J. Scalable Electron Correlation Methods. 3. Efficient and Accurate Parallel Local Coupled Cluster with Pair Natural Orbitals (PNO-LCCSD). *J. Chem. Theory Comput.* **2017**, *13*, 3650−3675.

(12) Ma, Q.; Werner, H.-J. Scalable Electron Correlation Methods. 5. Parallel Perturbative Triples Correction for Explicitly Correlated Local Coupled Cluster with Pair Natural Orbitals. *J. Chem. Theory Comput.* **2018**, *14*, 198−215.

(13) Schmitz, G.; Hättig, C.; Tew, D. P. Explicitly Correlated PNO-MP2 and PNO-CCSD and Their Application to the S66 Set and Large Molecular Systems. *Phys. Chem. Chem. Phys.* **2014**, *16*, 22167−22178.

(14) Schmitz, G.; Hättig, C. Perturbative Triples Correction for Local Pair Natural Orbital Based Explicitly Correlated CCSD(F12*) Using Laplace Transformation Techniques. *J. Chem. Phys.* **2016**, *145*, 234107.

(15) Schmitz, G.; Hättig, C. Accuracy of Explicitly Correlated Local PNO-CCSD(T). *J. Chem. Theory Comput.* **2017**, *13*, 2623−2633.

(16) Nagy, P. R.; Samu, G.; Kállay, M. Optimization of the Linear-Scaling Local Natural Orbital CCSD(T) Method: Improved Algorithm and Benchmark Applications. *J. Chem. Theory Comput.* **2018**, *14*, 4193−4215.

(17) Rolik, Z.; Szegedy, L.; Ladjánszki, I.; Ladóczki, B.; Kállay, M. An Efficient Linear-Scaling CCSD(T) Method Based on Local Natural Orbitals. *J. Chem. Phys.* **2013**, *139*, 094105.

(18) Nagy, P. R.; Kállay, M. Optimization of the Linear-Scaling Local Natural Orbital CCSD(T) Method: Redundancy-Free Triples Correction Using Laplace Transform. *J. Chem. Phys.* **2017**, *146*, 214106.

(19) Yang, J.; Kurashige, Y.; Manby, F. R.; Chan, G. K. L. Tensor factorizations of local second-order Møller-Plesset theory. *J. Chem. Phys.* **2011**, *134*, 044123.

(20) Kitaura, K.; Ikeo, E.; Asada, T.; Nakano, T.; Uebayasi, M. Fragment Molecular Orbital Method: An Approximate Computational Method for Large Molecules. *Chem. Phys. Lett.* **1999**, *313*, 701−706.

DOI: 10.1021/acs.jpca.9b08077
J. Phys. Chem. A XXXX, XXX, XXX−XXX

(21) Kitaura, K.; Sugiki, S.-I.; Nakano, T.; Komeiji, Y.; Uebayasi, M. Fragment Molecular Orbital Method: Analytical Energy Gradients. *Chem. Phys. Lett.* **2001**, *336*, 163−170.
(22) Li, W.; Piecuch, P.; Gour, J. R.; Li, S. Local Correlation Calculations Using Standard and Renormalized Coupled-Cluster Approaches. *J. Chem. Phys.* **2009**, *131*, 114109.
(23) Li, W.; Piecuch, P. Improved Design of Orbital Domains within the Cluster-in-Molecule Local Correlation Framework: Single-Environment Cluster-in-Molecule Ansatz and Its Application to Local Coupled-Cluster Approach with Singles and Doubles†. *J. Phys. Chem. A* **2010**, *114*, 8644−8657.
(24) Li, W.; Piecuch, P. Multilevel Extension of the Cluster-in-Molecule Local Correlation Methodology: Merging Coupled-Cluster and Møller−Plesset Perturbation Theories. *J. Phys. Chem. A* **2010**, *114*, 6721−6727.
(25) Friedrich, J.; Hanrath, M.; Dolg, M. Fully Automated Implementation of the Incremental Scheme: Application to CCSD Energies for Hydrocarbons and Transition Metal Compounds. *J. Chem. Phys.* **2007**, *126*, 154110.
(26) Friedrich, J.; Tew, D. P.; Klopper, W.; Dolg, M. Automated Incremental Scheme for Explicitly Correlated Methods. *J. Chem. Phys.* **2010**, *132*, 164114.
(27) Friedrich, J.; Walczak, K. Incremental CCSD(T)(F12)—MP2-F12—A Method to Obtain Highly Accurate CCSD(T) Energies for Large Molecules. *J. Chem. Theory Comput.* **2013**, *9*, 408−417.
(28) Li, W.; Li, S. Divide-and-Conquer Local Correlation Approach to the Correlation Energy of Large Molecules. *J. Chem. Phys.* **2004**, *121*, 6649−6657.
(29) Kobayashi, M.; Nakai, H. Divide-and-Conquer-Based Linear-Scaling Approach for Traditional and Renormalized Coupled Cluster Methods with Single, Double, and Noniterative Triple Excitations. *J. Chem. Phys.* **2009**, *131*, 114108.
(30) Förner, W.; Ladik, J.; Otto, P.; Cížek, J. Coupled-Cluster Studies. II. The Role of Localization in Correlation Calculations on Extended Systems. *Chem. Phys.* **1985**, *97*, 251−262.
(31) Förner, W. Coupled Cluster Studies. IV. Analysis of the Correlated Wavefunction in Canonical and Localized Orbital Casis for Ethylene, Carbon Monoxide, and Carbon Dioxide. *Chem. Phys.* **1987**, *114*, 21−35.
(32) Ziółkowski, M.; Jansík, B.; Kjærgaard, T.; Jørgensen, P. Linear Scaling Coupled Cluster Method with Correlation Energy Based Error Control. *J. Chem. Phys.* **2010**, *133*, 014107.
(33) Kristensen, K.; Høyvik, I.-M.; Jansik, B.; Jørgensen, P.; Kjærgaard, T.; Reine, S.; Jakowski, J. MP2 Energy and Density for Large Molecular Systems with Internal Error Control Using the Divide-Expand-Consolidate Scheme. *Phys. Chem. Chem. Phys.* **2012**, *14*, 15706.
(34) Kjaergaard, T.; Baudin, P.; Bykov, D.; Kristensen, K.; Jørgensen, P. The Divide-Expand-Consolidate Coupled Cluster Scheme. *Wiley Interdiscip. Rev.: Comput. Mol. Sci.* **2017**, *7*, No. e1319.
(35) Kjærgaard, T.; Baudin, P.; Bykov, D.; Eriksen, J. J.; Ettenhuber, P.; Kristensen, K.; Larkin, J.; Liakh, D.; Pawłowski, F.; Vose, A.; et al. Massively Parallel and Linear-Scaling Algorithm for Second-Order Møller−Plesset Perturbation Theory Applied to the Study of Supramolecular Wires. *Comput. Phys. Commun.* **2017**, *212*, 152−160.
(36) Høyvik, I.-M.; Jørgensen, P. Characterization and Generation of Local Occupied and Virtual Hartree-Fock Orbitals. *Chem. Rev.* **2016**, *116*, 3306−3327.
(37) Humbel, S.; Sieber, S.; Morokuma, K. The IMOMO Method: Integration of Different Levels of Molecular Orbital Approximations for Geometry Optimization of Large Systems: Test for n-Butane Conformation and S_N2 Reaction: RCl+Cl$^-$. *J. Chem. Phys.* **1996**, *105*, 1959−1967.
(38) Svensson, M.; Humbel, S.; Froese, R. D. J.; Matsubara, T.; Sieber, S.; Morokuma, K. ONIOM: A Multilayered Integrated MO + MM Method for Geometry Optimizations and Single Point Energy Predictions. A Test for Diels-Alder Reactions and Pt$(P(t\text{-}Bu)_3)_2$ + H_2 Oxidative Addition. *J. Phys. Chem.* **1996**, *100*, 19357−19363.
(39) Mata, R. A.; Werner, H.-J.; Schütz, M. Correlation Regions Within a Localized Molecular Orbital Approach. *J. Chem. Phys.* **2008**, *128*, 144106.
(40) Piecuch, P.; Włoch, M. Renormalized Coupled-Cluster Methods Exploiting Left Eigenstates of the Similarity-Transformed Hamiltonian. *J. Chem. Phys.* **2005**, *123*, 224105.
(41) Piecuch, P.; Włoch, M.; Gour, J. R.; Kinal, A. Single-Reference, Size-Extensive, Non-Iterative Coupled-Cluster Approaches to Bond Breaking and Biradicals. *Chem. Phys. Lett.* **2006**, *418*, 467−474.
(42) Sparta, M.; Retegan, M.; Pinski, P.; Riplinger, C.; Becker, U.; Neese, F. Multilevel Approaches within the Local Pair Natural Orbital Framework. *J. Chem. Theory Comput.* **2017**, *13*, 3198−3207.
(43) Hégely, B.; Nagy, P. R.; Kállay, M. Dual Basis Set Approach for Density Functional and Wave Function Embedding Schemes. *J. Chem. Theory Comput.* **2018**, *14*, 4600−4615.
(44) Baudin, P.; Ettenhuber, P.; Reine, S.; Kristensen, K.; Kjærgaard, T. Efficient Linear-Scaling Second-Order Møller-Plesset Perturbation Theory: The Divide-Expand-Consolidate RI-MP2 Model. *J. Chem. Phys.* **2016**, *144*, 054102.
(45) Kjærgaard, T. The Laplace Transformed Divide-Expand-Consolidate Resolution of the Identity Second-Order Møller-Plesset Perturbation (DEC-LT-RIMP2) Theory Method. *J. Chem. Phys.* **2017**, *146*, 044103.
(46) Rosi, N. L.; Kim, J.; Eddaoudi, M.; Chen, B.; O'Keeffe, M.; Yaghi, O. M. Rod Packings and Metal-Organic Frameworks Constructed from Rod-Shaped Secondary Building Units. *J. Am. Chem. Soc.* **2005**, *127*, 1504−1518.
(47) Wu, H.; Zhou, W.; Yildirim, T. High-Capacity Methane Storage in Metal-Organic Frameworks M2 (dhtp): The Important Role of Open Metal Sites. *J. Am. Chem. Soc.* **2009**, *131*, 4995−5000.
(48) Wu, H.; Simmons, J. M.; Srinivas, G.; Zhou, W.; Yildirim, T. Adsorption Sites and Binding Nature of CO_2 in Prototypical Metal-Organic Frameworks: A Combined Neutron Diffraction and First-Principles Study. *J. Phys. Chem. Lett.* **2010**, *1*, 1946−1951.
(49) Geier, S. J.; Mason, J. A.; Bloch, E. D.; Queen, W. L.; Hudson, M. R.; Brown, C. M.; Long, J. R. Selective adsorption of ethylene over ethane and propylene over propane in the metal-organic frameworks M2(dobdc) (M = Mg, Mn, Fe, Co, Ni, Zn). *Chem. Sci.* **2013**, *4*, 2054−2061.
(50) Magdysyuk, O. V.; Adams, F.; Liermann, H.-P.; Spanopoulos, I.; Trikalitis, P. N.; Hirscher, M.; Morris, R. E.; Duncan, M. J.; McCormick, L. J.; Dinnebier, R. E. Understanding the Adsorption Mechanism of Noble Gases Kr and Xe in CPO-27-Ni, CPO-27-Mg, and ZIF-8. *Phys. Chem. Chem. Phys.* **2014**, *16*, 23908−23914.
(51) Tan, K.; Zuluaga, S.; Wang, H.; Canepa, P.; Soliman, K.; Cure, J.; Li, J.; Thonhauser, T.; Chabal, Y. J. Interaction of Acid Gases SO2 and NO2 with Coordinatively Unsaturated Metal Organic Frameworks: M-MOF-74 (M = Zn, Mg, Ni, Co). *Chem. Mater.* **2017**, *29*, 4227−4235.
(52) *LSDalton: A Linear Scaling Molecular Electronics Strucutre Program*. http://daltonprogram.org, 2016.
(53) Aidas, K.; Angeli, C.; Bak, K. L.; Bakken, V.; Bast, R.; Boman, L.; Christiansen, O.; Cimiraglia, R.; Coriani, S.; Dahle, P.; et al. The Dalton Quantum Chemistry Program System. *Wiley Interdiscip. Rev.: Comput. Mol. Sci.* **2014**, *4*, 269−284.
(54) Pipek, J.; Mezey, P. G. A Fast Intrinsic Localization Procedure Applicable for Ab Initio and Semiempirical Linear Combination of Atomic Orbital Wave Functions. *J. Chem. Phys.* **1989**, *90*, 4916−4926.
(55) Boys, S. F. Construction of Some Molecular Orbitals to Be Approximately Invariant for Changes from One Molecule to Another. *Rev. Mod. Phys.* **1960**, *32*, 296−299.
(56) Jansík, B.; Høst, S.; Kristensen, K.; Jørgensen, P. Local Orbitals by Minimizing Powers of the Orbital Variance. *J. Chem. Phys.* **2011**, *134*, 194104.
(57) Høyvik, I.-M.; Jansik, B.; Jørgensen, P. Orbital Localization Using Fourth Central Moment Minimization. *J. Chem. Phys.* **2012**, *137*, 224114.

DOI: 10.1021/acs.jpca.9b08077
J. Phys. Chem. A XXXX, XXX, XXX−XXX

(58) Ettenhuber, P.; Baudin, P.; Kjærgaard, T.; Jørgensen, P.; Kristensen, K. Orbital Spaces in the Divide-Expand-Consolidate Coupled Cluster Method. *J. Chem. Phys.* **2016**, *144*, 164116.
(59) Becke, A. D. Density-Functional Exchange-Energy Approximation with Correct Asymptotic Behavior. *Phys. Rev. A: At., Mol., Opt. Phys.* **1988**, *38*, 3098−3100.
(60) Perdew, J. P. Density-Functional Approximation for the Correlation Energy of the Inhomogeneous Electron Gas. *Phys. Rev. B* **1986**, *33*, 8822−8824.
(61) Valiev, M.; Bylaska, E. J.; Govind, N.; Kowalski, K.; Straatsma, T. P.; Van Dam, H. J. J.; Wang, D.; Nieplocha, J.; Apra, E.; Windus, T. L.; et al. NWChem: A Comprehensive and Scalable Open-Source Solution for Large Scale Molecular Simulations. *Comput. Phys. Commun.* **2010**, *181*, 1477−1489.
(62) Yazaydın, A. Ö.; Snurr, R. Q.; Park, T.-H.; Koh, K.; Liu, J.; LeVan, M. D. Screening of Metal-Organic Frameworks for Carbon Dioxide Capture from Flue Gas Using a Combined Experimental and Modeling Approach. *J. Am. Chem. Soc.* **2009**, *131*, 18198−18199.
(63) Lee, K.; Howe, J. D.; Lin, L.-C.; Smit, B.; Neaton, J. B. Small-Molecule Adsorption in Open-Site Metal-Organic Frameworks: A Systematic Density Functional Theory Study for Rational Design. *Chem. Mater.* **2015**, *27*, 668−678.
(64) Yu, K.; Kiesling, K.; Schmidt, J. R. Trace Flue Gas Contaminants Poison Coordinatively Unsaturated Metal-Organic Frameworks: Implications for CO2 Adsorption and Separation. *J. Phys. Chem. C* **2012**, *116*, 20480−20488.

DOI: 10.1021/acs.jpca.9b08077
J. Phys. Chem. A XXXX, XXX, XXX−XXX